Resonant states 3^+ and 2^- of the Boron isotope ^{8}B

T. J. Tshipi*, S. A. Rakityansky*,†,‡ and S. N. Ershov†,§

*Department of Physics, University of Pretoria, Pretoria, South Africa

†Joint Institute for Nuclear Research, Dubna, Russia

‡rakitsa@theor.jinr.ru

§ershov@theor.jinr.ru

Received 5 May 2022
Revised 23 June 2022
Accepted 12 July 2022
Published 13 August 2022

The Jost functions, constructed by fitting available partial cross-sections for the elastic $p\,^7$Be scattering with $J^\pi = 3^+, 2^-$, are analytically continued to complex energies, where the resonances are located as their zeros. In addition to the resonance energies and widths, the residues of the S-matrix at the corresponding poles, as well as the Asymptotic Normalization Constants (ANC) are determined. The fitting is done using the semi-analytic representation of the Jost function with proper analytic structure, defined on the Riemann surface whose topology involves not only the square-root but also the logarithmic branching caused by the Coulomb interaction.

Keywords: Jost matrix; quantum resonances; analytic continuation; Coulomb interaction.

PACS Number(s): 03.65.Nk, 11.55.Bq, 13.85.Dz, 21.10.−k, 21.10.Tg, 27.20.+n

1. Introduction

The nucleus ^{8}B plays an important role in nuclear astrophysics. In particular, the rediative capture $^7\mathrm{Be}(p,\gamma)^8\mathrm{B}$ is one of the reactions constituting the pp-chain.[1] It is therefore necessary to have a good knowledge and a reliable understanding of all the properties of this eight-body nuclear system. This requires the development of various theoretical models of it as well as the corresponding experimental studies and based on them phenomenological analyses of the data.

So far, most of the theoretical studies were focused on the ground-state properties of ^{8}B and on calculating the astrophysical factor, S_{17}, that is crucial for describing various processes induced by proton-^{7}Be collisions at extremely low energies. As far as the excited states (i.e., the resonances) of ^{8}B are concerned, very few

‡Corresponding author.

theoretical works were devoted to such a problem. The theoretical treatments of ^{8}B vary from the so-called *ab initio* calculations to some semi-phenomenological approaches. These treatments include but not limited to the quantum Monte Carlo calculations,[2] no-core, Gamow, and realistic shell models,[3–5] a variety of microscopic cluster,[6] potential[7] models, etc. Within some of these approaches (see Refs. 8 and 9) in addition to calculations of the low-energy ^{8}B spectrum, the widths of the low-lying resonances are evaluated.

The most reliable knowledge on the spectrum of ^{8}B is accumulated from the measurements of the elastic and inelastic scattering of protons from ^{7}Be in conjunction with phenomenological analyses based on the R-matrix theory. Recently, it was suggested to complement the R-matrix approach by a new method based on the Jost-matrix parametrization, which offers an alternative way of analytic continuation of the scattering data to the domain of complex energies (see Refs. 10–14). In particular, Ref. 13 was devoted to locating the resonant state 0^+ of the Boron isotope ^{8}B using the corresponding R-matrix data within that new approach. This work is yet another application of such a parametrization for re-examining the locations of two more resonances in ^{8}B, namely, the states 3^+ and 2^-.

The p^7Be-threshold is just $\sim$ 138 keV above the ground state of ^{8}B.[15] This means that the proton is loosely bound and thus the two-body model, $p + {}^7$Be, should be good enough for describing the low-lying excited states of ^{8}B as well as the low-energy p^7Be-scattering. Such a model needs the corresponding two-body potential, which could be constructed based on available experimental data. An example of such a potential can be found in Ref. 7.

The resonances that are formed in the p^7Be-collisions, are among the important data which are needed to construct a phenomenological potential. The R-matrix analysis[16] of the elastic and inelastic proton-^{7}Be scattering at the collision energies between 1.6 MeV and 3.4 MeV, provides the energies and widths of several low-lying resonances. Any additional test or confirmation of these resonance parameters would be useful and valuable. Doing such a test was the main goal of our present work.

We use here the partial cross-sections in the states 3^+ and 2^-, obtained from the R-matrix of Ref. 16, and construct the corresponding Jost functions with proper analytic structure. Examining these Jost functions at complex energies, we determine the parameters of the resonances. In this way, we actually do an analytic continuation of the scattering data available on the real axis. It is done to check if the proper analytic continuation can give the parameters different from those obtained in Ref. 16. It turned out that we obtained slightly different resonance energies and widths.

In addition to the resonance energies and widths, we also determine the residues of the S-matrix at the corresponding poles as well as the Asymptotic Normalization Coefficients (ANC) of the resonance wave functions. The ANC's determine the behavior of these functions at large distances that give major contribution to the processes of radiative capture (see, for example, Ref. 17 which is rather old

but very pedagogical). The knowledge of them is therefore important for nuclear astrophysics. To the best of our knowledge there are no reported values of the ANC's for the states 3^+ and 2^- of ^{8}B.

This work is a continuation of our previous publications,[10–14,18,19] where the reader can find all the details of the method we use here. To avoid the unnecessary repetition, we therefore present it rather briefly.

2. Parametrization of the *S*-Matrix

When proton collides with the nucleus ^{7}Be at the energies greater than 0.4291 MeV, this target nucleus can transit from its ground state with the spin 3/2 and negative parity to the first excited state with the spin 1/2 and also negative parity.[20] The

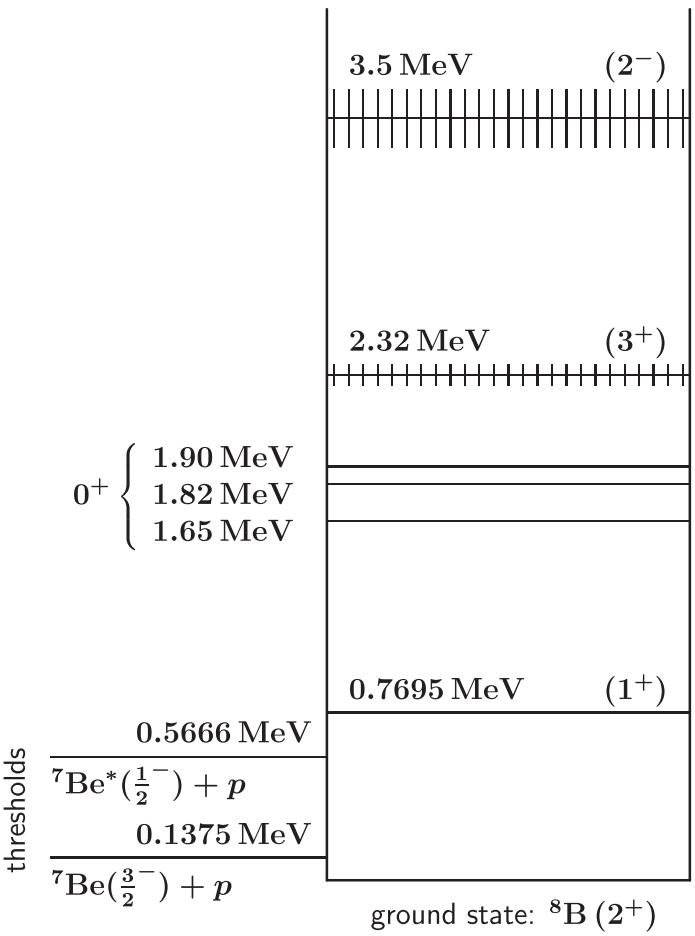

Fig. 1. Known low-energy resonances in the nuclear system ^{8}B. The data are taken from Refs. 13,15 and 16. For the state 0^+ Ref. 16 gives the energy of 1.90 MeV while in Ref. 13 two overlapping resonances at the energies of 1.65 MeV and 1.82 MeV are found.

Table 1. Coupled partial waves in the p^7Be-collision for the states 3^+ and 2^-. Here, ℓ is the relative orbital angular momentum, and s is the total spin of the proton-Beryllium system.

J^π	(ℓ, s) for $p\,^7\mathrm{Be}(\frac{3}{2}^-)$	(ℓ, s) for $p\,^7\mathrm{Be}^*(\frac{1}{2}^-)$
3^+	$(1,2)$, $(3,1)$, $(3,2)$, $(5,2)$	$(3,0)$, $(3,1)$
2^-	$(0,2)$, $(2,1)$, $(2,2)$, $(4,2)$	$(2,0)$, $(2,1)$

spectrum of known excited states of the corresponding compound nucleus, ^{8}B, is shown in Fig. 1.

The possibility of exciting the target means that in such a collision there are two channels with different thresholds. Each of these channels consists of a number of partial waves (degenerate sub-channels). Since the total angular momentum J and the parity π are conserving, the number of coupled partial waves is limited. For the states with J^π equal to 3^+ and 2^- (which we consider in this work), all possible combinations (ℓ, s) of the orbital angular momentum ℓ and the total spin s of ^{8}B are listed in Table 1.

As is seen, formally, there are six coupled channels for both states. As usual in such a case, in order to simplify the problem, we assume that the partial waves with the minimal values of ℓ are dominant (because the higher centrifugal barriers in the other partial waves make the formation of the resonances less probable). Such a reasonable assumption allows us to ignore all the higher partial waves and to consider the single-channel problems for both the 3^+ and 2^- states, namely, the partial waves $(1,2)$ and $(0,2)$.

The corresponding single-channel S-matrix at the energy E can be expressed via the Jost functions $f_\ell^{(\mathrm{in/out})}$ (see, for example, Ref. 18),

$$S_\ell(E) = f_\ell^{(\mathrm{out})}(E)[f_\ell^{(\mathrm{in})}(E)]^{-1}, \tag{1}$$

where in order to simplify notations, we drop the symbols J and π. For the Jost functions in the above equation, we use the following exact semi-analytic expressions obtained in Ref. 18:

$$f_\ell^{(\mathrm{in/out})}(E) = \frac{e^{\pi\eta/2}\ell!}{\Gamma(\ell+1\pm i\eta)}\left\{A_\ell(E) - \left[\frac{2\eta h(\eta)}{C_0^2(\eta)} \pm i\right] C_\ell^2(\eta) k^{2\ell+1} B_\ell(E)\right\}, \tag{2}$$

where k is the wave number related to the collision (c.m.) energy as

$$k = \pm\sqrt{2\mu E/\hbar^2}, \tag{3}$$

with μ being the reduced mass, $C_\ell(\eta)$ is the Coulomb barrier factor depending on the Sommerfeld parameter η,

$$C_\ell(\eta) = \frac{2^\ell e^{-\pi\eta/2}}{(2\ell)!!}\exp\left\{\frac{1}{2}[\ln\Gamma(\ell+1+i\eta) + \ln\Gamma(\ell+1-i\eta)]\right\} \underset{\eta\to 0}{\longrightarrow} 1 \tag{4}$$

and

$$h(\eta) = \frac{1}{2}[\psi(i\eta) + \psi(-i\eta)] - \ln\eta, \quad \psi(z) = \frac{\Gamma'(z)}{\Gamma(z)}, \quad \eta = \frac{e^2 Z_1 Z_2 \mu}{\hbar^2 k}. \tag{5}$$

The only unknown quantities in Eq. (2) are the functions $A_\ell(E)$ and $B_\ell(E)$ which are determined by the dynamics of the physical system.

As is seen, the S-matrix is not a single-valued function of the variable E. This is because the Jost functions depend on the energy via the momentum, k, and its logarithm, $\ln(k)$. For a single value of variable E, the momentum has two different values depending on the choice of sign in front of the square root (3), while its logarithm has infinitely many different values. This means that the S-matrix is defined on a spiral Riemann surface, where the threshold energy, $E = 0$, is the branch point of the square-root and the logarithm type at the same time (see, Refs. 12 and 13).

As is shown in Ref. 18, the functions $A_\ell(E)$ and $B_\ell(E)$ are single-valued analytic functions of the energy. They are defined on a simple energy plane without any branch points. All the complications related to the multi-valuedness of the S-matrix and branching of the Riemann surface are caused by the explicit factors in the representations (2).

It should be noted that these representations are exact, i.e., they are rigorously derived from the Schrödinger equation. They are valid for any two-body system. In a sense, all the explicit factors in them are determined by the kinematics, while the unknown functions $A_\ell(E)$ and $B_\ell(E)$ describe the dynamics of a specific system. Apparently, these functions are more simple because they are single-valued.

If we use any (reasonable) approximations for the functions $A_\ell(E)$ and $B_\ell(E)$, the proper analytic structure of the S-matrix remains correct, i.e., the exact explicit factors in (2) remain intact and thus correctly describe topology of the Riemann surface. Having the correct analytic structure of the S-matrix is important when it is analytically continued from the real axis to complex energies in search for possible resonances.

Since they are analytic, as an approximation of the functions $A_\ell(E)$ and $B_\ell(E)$, we can take the first few terms of their expansions in the Taylor series around an arbitrary complex point E_0,

$$A_\ell(E) \approx a_\ell^{(0)} + a_\ell^{(1)}(E - E_0) + a_\ell^{(2)}(E - E_0)^2 + \cdots + a_\ell^{(M)}(E - E_0)^M, \qquad (6)$$

$$B_\ell(E) \approx b_\ell^{(0)} + b_\ell^{(1)}(E - E_0) + b_\ell^{(2)}(E - E_0)^2 + \cdots + b_\ell^{(M)}(E - E_0)^M. \qquad (7)$$

The unknown expansion coefficients $a_\ell^{(n)}$ and $b_\ell^{(n)}$ can be used as the free paremeters in fitting a set of experimental data. In Ref. 18, it is shown that these parametes are real, if the central point E_0 is chosen on the real axis.

Here, we use the same fitting procedure as was described in Refs. 10–14 and 19. The point E_0 is taken somewhere within the energy interval, for which the data points for the cross-section in partial wave ℓ are available. The optimal values of the unknown parameters $a_\ell^{(n)}$ and $b_\ell^{(n)}$ are found by minimizing the deviations of the theoretical cross-section curve (obtained using the S-matrix (1)) from the data points.

When the optimal values of these parameters are found, we have a reliable approximation for the S-matrix (1) with the correct analytic properties. This S-matrix can be used at complex energies within a circle around E_0. The more terms are used in the Taylor expansions (6) and (7), the bigger is the radius of that circle. The resonances can be found as zeros of the Jost function

$$f_\ell^{(\mathrm{in})}(E) = 0, \tag{8}$$

on the nonphysical sheet of the Riemann surface. Choice of the sheet is done by choosing the appropriate sign in Eq. (3).

The poles of the S-matrix are simple. Therefore, the residues of the S-matrix can be found by numerical differentiation of the Jost function $f_\ell^{(\mathrm{in})}(E)$ in the denominator of Eq. (1), as described in Ref. 13. Such a residue determines the asymptotic normalization coefficient, $\mathcal{A}_\ell$, of the radial part, $u_\ell(E,r)$, of the wave function

$$\psi_\ell(E,\vec{r}) = \frac{u_\ell(E,r)}{r} Y_{\ell m}(\Omega), \quad u_\ell(E,r) \underset{r\to\infty}{\longrightarrow} \mathcal{A}_\ell e^{ikr - i\eta \ln(2kr)}. \tag{9}$$

A derivation of the corresponding relation

$$\mathrm{Res}[S_\ell, E] = i(-1)^{\ell+1} \frac{\hbar^2 k}{\mu} \mathcal{A}_\ell^2, \tag{10}$$

can be found, for example, in Ref. 14.

3. Results and Discussion

As the data points to fit, we use the partial cross-sections in the channels 3^+ and 2^-, which we calculated with the help of the R-matrix published in Ref. 16. Since these cross-sections are smooth theoretical curves, we can choose any number of points and distribute them as we need within the energy interval where the given R-matrix is reliable.

A possible question about the absence of error-bars in the data was discussed several times in our previous publications (see Refs. 10–14). In particular, in Ref. 10, using single- and two-channel models where the exact resonance parameters were known, it was demonstrated that these parameters could be accurately reproduced when the data had some error bars. In Ref. 11, we studied how the accuracy of our analytic continuation depends on the size of the experimental errors. It was found that the method is very stable and some inaccuracies only appear if the error bars become huge.

In principle, the proposed parametrization could be used to analyze any raw experimental data. However, in its present form, we apply the method as complimentary (secondary) one to the R-matrix analysis. Within the R-matrix approach, it is possible to do very accurate analysis of the data on the real axis (for real collision energies). Using of the same parametrization outside the real axis is not rigorously substantiated. This is especially true when the Coulomb forces are present and the Riemann surface has complicated topology. Our main task in this work

was to check how a proper analytic structure of the parametrization used for the analytic continuation, could influence the results. For the purpose of the correct comparison, we therefore had to use the same partial cross-sections that follow from the R-matrix analysis, i.e., the same curves that correspond to the R-matrix parameters. These parameters have definite values and thus the cross-section curves have no uncertainties. In a sense, this formally means that we use uniform (equal) error-bars for all the data points. In such a case they are reduced to a common normalization factor in the goal-function (chi-square) that we minimize, and therefore do not influence either the minimization procedure or its results.

The cross-sections, we obtained from the R-matrix of Ref. 16, are given in Figs. 2 and 3, where they are shown by the dots. We consider these dots as the (indirectly obtained) "experimental" points, which we fit by varying the parameters $a_\ell^{(n)}(E_0)$ and $b_\ell^{(n)}(E_0)$ in Eqs. (6) and (7) that determine the Jost functions.

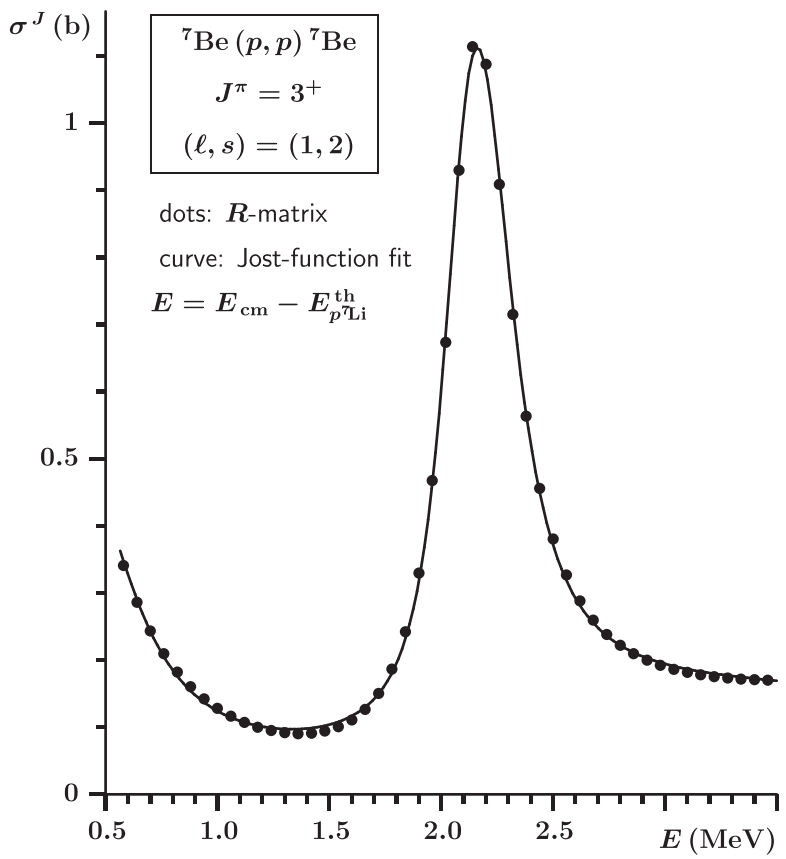

Fig. 2. Partial cross-section for the elastic p^7Be scattering in the state with $J^\pi = 3^+$. The dots are the "experimental" points obtained from the R-matrix taken from Ref. 16. The curve is our fit with the Jost function parameters given in Table 2. The collision energy is counted from p^7Be threshold energy $E^{\rm th}_{p^7{\rm Be}} = 0.1375\,{\rm MeV}$.

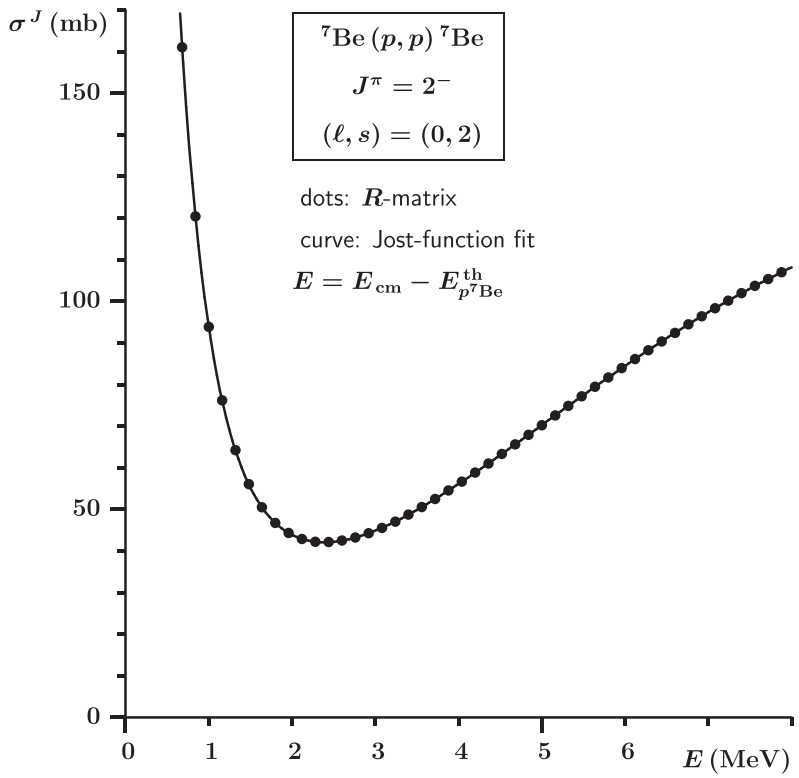

Fig. 3. Partial cross-section for the elastic p^7Be scattering in the state with $J^\pi = 2^-$. The dots are the "experimental" points obtained from the R-matrix taken from Ref. 16. The curve is our fit with the Jost function parameters given in Table 3. The collision energy is counted from p^7Be threshold energy $E^{\rm th}_{p^7{\rm Be}} = 0.1375\,{\rm MeV}$.

For the state 3^+, we use $E_0 = 2.0\,{\rm MeV}$ (counted from p^7Be-threshold) and $M = 4$. The resonance in the state 2^- was expected to be found at around $\sim 3.5\,{\rm MeV}$ and with a much larger width. This means that the corresponding pole of the S-matrix is at a larger distance from the real axis. In order to have a wider circle where the Taylor expansions (6) and (7) could be valid, we use more terms in them, namely, $M = 7$ for the state 2^-. The central point in these expansions for this state is chosen at $E_0 = 3.2\,{\rm MeV}$.

In order to minimize the deviations of our theoretical curves (partial cross-sections) from the data points, we use the MINUIT program developed in CERN.[21] Thus found optimal values of the fitting parameters for the states 3^+ and 2^- are presented in Tables 2 and 3, respectively. The corresponding theoretical curves are shown in Figs. 2 and 3.

It should be noted that the cross-sections (as well as any other observables) are expressed via the S-matrix (1), i.e., via the ratio of the Jost functions. In such a ratio, any common factor in $f^{(\rm in)}_\ell$ and $f^{(\rm out)}_\ell$ cancels out. This means that the set of

Table 2. Parameters of the expansions (6) and (7) for the state 3^+ with $M = 4$ and with the central point $E_0 = 2.0\,\mathrm{MeV}$ (counted from p^7Be-threshold). These parameters were used to generate the curve shown in Fig. 2.

n	$a_\ell^{(n)}$ $[\mathrm{MeV}^{-n}]$	$b_\ell^{(n)}$ $[\mathrm{fm}^3 \cdot \mathrm{MeV}^{-n}]$
0	1.0000	38.588
1	−1.4127	49.551
2	7.4547	−7.3743
3	11.577	205.77
4	3.7367	−13.477

Table 3. Parameters of the expansions (6) and (7) for the state 2^- with $M = 7$ and with the central point $E_0 = 3.2\,\mathrm{MeV}$ (counted from p^7Be-threshold). These parameters were used to generate the curve shown in Fig. 3.

n	$a_\ell^{(n)}$ $[\mathrm{MeV}^{-n}]$	$b_\ell^{(n)}$ $[\mathrm{fm} \cdot \mathrm{MeV}^{-n}]$
0	1.00000	−0.47918
1	0.31405	−0.84971
2	0.18989×10^{-1}	−0.11307
3	0.22203×10^{-1}	-0.29998×10^{-1}
4	-0.16700×10^{-1}	-0.41213×10^{-2}
5	-0.10862×10^{-1}	0.17864×10^{-1}
6	-0.96436×10^{-3}	0.57073×10^{-2}
7	0.90906×10^{-4}	0.21659×10^{-3}

the parameters $a_\ell^{(n)}$ and $b_\ell^{(n)}$ can be scaled by any convenient factor. Such a scaling does not affect any results. In particular, we can always fix the value of one of the parameters during the minimization procedure. This is why in both Tables 2 and 3 we have $a_\ell^{(0)} = 1$. The units for the parameters are chosen in such a way that the Jost matrices are dimensionless.

Having found (by fitting the data) the optimal values of $a_\ell^{(n)}$ and $a_\ell^{(n)}$, we may use the resulting Jost functions (2) at complex energies within a circle where the truncated series (6) and (7) are sufficiently accurate. By doing this, we actually do analytic continuation of the Jost functions from the real axis (where they reproduce available data) to the domain of complex energies where we can look for resonances as the roots of Eq. (8). These roots correspond to the poles of the S-matrix (1). The results of such a search are given in Table 4, where in addition to the resonance energies and widths the corresponding residues of the S-matrix and the Asymptotic Normalization Coefficients of the resonance wave functions are presented.

Comparing the resonance energy and width given in Table 4 for the state 3^+ with the corresponding results obtained in Ref. 16

$$E_\mathrm{r}(3^+) = (2.32 \pm 0.02) - \frac{i}{2}(0.33 \pm 0.03)\ \mathrm{MeV}, \quad \text{Ref. 16}, \tag{11}$$

Table 4. Resonance energies, the residues of the S-matrix at the corresponding poles, and the Asymptotic Normalization Coefficients of the resonance wave functions for the states 3^+ and 2^- of ^{8}B, obtained in this work with the help of analytic continuation of the Jost functions. The energy $E_{\rm r}$ is counted from the ground state of ^{8}B.

^{8}B	$E_{\rm r}$ [MeV]	Res$[S_\ell, E_{\rm r}]$ [MeV]	ANC [fm$^{-1/2}$]
3^+	$2.22 - \frac{i}{2}0.369$	$-0.106 - i0.0561$	0.0924
2^-	$3.66 - \frac{i}{2}4.70$	$(0.365 - i1.02) \times 10^{-3}$	7.34×10^{-3}

we see that our numbers are not far but a bit outside one standard deviation. This is despite the fact that we base our analysis on the same data taken on the real axis of the energy variable. The difference emphasizes the importance of using a parametrization with a proper analytic structure when a complex function is analytically continued.

As to the state 2^-, our results for the resonance energy and width are well within the standard deviation intervals of the corresponding evaluation given in Ref. 15, namely,

$$E_{\rm r}(2^-) = (3.5 \pm 0.5) - \frac{i}{2}(8 \pm 4)\ \text{MeV}, \quad \text{Ref. 15.} \tag{12}$$

In summary: Taking the data on the elastic scattering ^{7}Be$(p,p)^7$Be in the states 3^+ and 2^-, we performed analytic continuation of the corresponding Jost functions from the real energy axis to the nonphysical sheet of the Riemann surface where located one resonance in each of these states. The resonance energies and widths that we found turned out to be close to the values known before. However, in the case of the state 3^+, where previous evaluation of the resonance parameters was based on exactly the same data, we found a noticeable difference which indicates the importance of preserving proper analytic structure of the S-matrix when the analytic continuation is performed. In contrast to all previous analyses, we found not only the energies and widths of the resonances but also the residues of the S-matrix at the corresponding poles and the ANC of the resonance wave functions that could be used, for example, in calculations of electromagnetic transitions involving these resonances.

References

1. C. E. Rolfs and W. S. Rodney, *Cauldrons in the Cosmos* (The University of Chicago Press, Chicago and London, 1988).
2. G. B. King, L. Andreoli, S. Pastore, M. Piarulli, R. Schiavilla, R. B. Wiringa, *Phys. Rev. C* **102** (2020) 025501.
3. P. Maris, J. P. Vary and P. Navrátil, *Phys. Rev. C* **87** (2013) 014327.
4. X. Mao, J. Rotureau, W. Nazarewicz, N. Michel, R. M. Id Betan and Y. Jaganathen, *Phys. Rev. C* **102** (2020) 024309.
5. T. Fukui, L. De Angelis, Y. Z. Ma, L. Coraggio, A. Gargano, N. Itaco and F. R. Xu, *Phys. Rev. C* **98** (2018) 044305.

6. P. Descouvemont, *Phys. Rev. C* **70** (2004) 065802.
7. S. B. Dubovichenko, N. A. Burkova, A. V. Dzhazairov-Kakhramanov and A. S. Tkachenko, *Nucl. Phys. A* **983** (2019) 175.
8. K. M. Nollett, *Phys. Rev. C* **86** (2012) 044330.
9. N. K. Timofeyuk, *Phys. Rev. C* **92** (2015) 034330.
10. S. A. Rakityansky and N. Elander, *Int. J. Mod. Phys. E* **22** (2013) 1350032.
11. P. Vaandrager and S. A. Rakityansky, *Int. J. Mod. Phys. E* **25** (2016) 1650014.
12. S. A. Rakityansky and S. N. Ershov, *Int. J. Mod. Phys. E* **28** (2019) 1950064.
13. S. A. Rakityansky, S. N. Ershov and T. J. Tshipi, *Int. J. Mod. Phys. E* **28** (2019) 1950083.
14. P. Vaandrager and S. A. Rakityansky, *Nucl. Phys. A* **992** (2019) 121627.
15. D. R. Tilley *et al.*, *Nucl. Phys. A* **745** (2004) 155.
16. J. P. Mitchell, G. V. Rogachev, E. D. Johnson, L. T. Baby, K. W. Kemper, A. M. Moro, P. Peplowski, A. S. Volya and I. Wiedenhover, *Phys. Rev. C* **87** (2013) 054617.
17. A. M. Mukhamedzhanov and R. E. Tribble, *Phys. Rev. C* **59** (1999) 3418.
18. S. A. Rakityansky and N. Elander, *J. Math. Phys. A* **54** (2013) 122112.
19. S. A. Rakityansky and N. Elander, *Few-Body Syst.* **54** (2013) 673.
20. D. R. Tilley *et al.*, *Nucl. Phys. A* **708** (2002) 3.
21. F. James and M. Roos, *Comput. Phys. Commun.* **10** (1975) 343, http://hep.fi.infn.it/minuit.pdf.